

Supplementary Information

A Dynamic DNA Nanosponge for Triggered Amplification of Gene-Photodynamic Modulation

Dan Luo,[‡] Xue Lin,[‡] Yun Zhao, Jialing Hu, Fengye Mo, Gege Song, Zhiqiao Zou, Fuan Wang, and Xiaoqing Liu*

College of Chemistry and Molecular Sciences, Wuhan University, Wuhan 430072, P. R. China.

* E-mail: xiaoqingliu@whu.edu.cn.

[‡] These authors contributed equally to this work.

Table of Contents

Supplemental Experimental Procedures	S1
Figure S1. Structure of porphyrin photosensitizer (TMPyP4)	S10
Table S1. DNA sequences	S11
Table S2. DLS measurement of different nanoassemblies	S12
Table S3. Calculation of replicated copies of DNA nanoassemblies	S13
Figure S2. EDX spectra of ADM	S14
Figure S3. X-ray photoelectron spectroscopy of ADMP	S15
Table S4. Calculation of photosensitizer loading capability and encapsulation efficiency ..	S16
Table S5. DLS analysis of stability in biological environments	S17
Figure S4. PAGE analysis of stability in biological environment	S18
Figure S5. ICP-MS analysis of responsive Mn ²⁺ release	S19
Figure S6. AD-mediated DNAzyme catalytic efficiency with Mg ²⁺ ions.....	S20
Figure S7. AD-mediated DNAzyme catalytic efficiency with Mn ²⁺ ions.....	S21
Figure S8. ADM-mediated DNAzyme catalytic efficiency	S22
Figure S9. Electron spin resonance analysis of ROS species.....	S23
Figure S10. ¹ O ₂ generation from irradiated ADMP	S24
Figure S11. ¹ O ₂ generation efficiency measurements	S25
Figure S12. Specific cancer cell recognition.....	S26
Figure S13. AS1411-mediated cellular uptake by 4T1 cells.....	S27
Figure S14. Colocalization analysis of 4T1 cells incubated with Cy5-labeled ADMP	S28
Figure S15. Biocompatibility of AmutDMP <i>in vitro</i>	S29
Figure S16. Cell viability of ADMP	S30
Figure S17. <i>In vivo</i> fluorescence imaging	S31
Figure S18. Weight of mice with different treatments	S32
Figure S19. Hemolysis test.....	S33
Figure S20. H&E staining of major organs	S34
Figure S21. Blood biochemical analyses	S35
References	S36

Supplemental Experimental Procedures

Materials. All high-performance liquid chromatography (HPLC)-purified oligonucleotides were used in this work (**Table S1**) and deoxynucleotides (dNTPs) solution mix were synthesized by Sangon Biotechnology (Shanghai, China). Stock solutions of DNA were prepared with phosphate buffer (PB) (20 mM, pH 7.0) and stored at -20 °C. T4 DNA ligase was purchased from New England Biolabs (Beverly, MA, USA). Phi29 DNA polymerase and LysoTracker Green were obtained from Thermo Fisher Scientific, Inc. (Waltham, MA, USA). 5,10,15,20-Tetrakis-(N-methyl-4-pyridyl)-porphine (TMPyP4), 1,3-diphenylisobenzofuran (DPBF), and Cyanine 5-dCTP (Cy5-dCTP) were purchased from Sigma-Aldrich (MO, USA). 2,2,6,6-Tetramethylpiperidine (TEMP), 5,5-Dimethyl-1-pyrroline N-oxide (DMPO) and Bovine serum albumin (BSA) were purchased from Aladdin Biochemical Technology Co., Ltd. (Shanghai, China). Potassium permanganate (KMnO₄), and H₂O₂ (30%, w/w) were purchased from Sinopharm Chemical Reagent Co., Ltd. (Shanghai, China). 30% Acrylamide/bis solution (29:1), Tris/Borate/EDTA (TBE) buffer, Tris/glycine/SDS (TGS) buffer, Gel-Red, and Coomassie brilliant blue were purchased from Bio-Rad (USA). 2',7'-dichlorofluorescein diacetate (DCFH-DA), annexin V-FITC/PI cell apoptosis kit, 4',6-diamidino-2-phenylindole (DAPI), and cell counting kit-8 (CCK-8) were obtained from Beyotime Biotechnology Co., Ltd. (Shanghai, China). A Calcein-AM/PI double-stain kit was purchased from Yeasen Biotechnology Co., Ltd. (Shanghai, China). Dulbecco's modified Eagle's medium (DMEM), fetal bovine serum (FBS), penicillin/streptomycin, trypsin, and Dulbecco's phosphate buffered saline (PBS) were purchased from GIBCO Invitrogen Corp. All reagents were analytical grade and used without any further purification. Ultrapure water used throughout the study was obtained from a Milli-Q apparatus (Millipore, Bedford, MA).

Instruments. UV-vis absorption spectra were recorded by UV-2600 UV-vis spectrophotometer (Shimadzu, Tokyo, Japan). Dynamic light scattering (DLS) analysis was carried out on Zetasizer (Nano-ZS90, Malvern, UK). A field-emission scanning electron microscope (Zeiss Merlin Compact) was used for SEM images. Elemental analysis and binding energy measurements were performed by X-ray Photoelectron Spectrometer (ESCALAB250Xi, Thermo Fisher Scientific, USA). Electron spin resonance (ESR) spectroscopy were measured by electron paramagnetic resonance spectrometer (Bruker A200, Bruker, Germany). Fluorescent spectra were measured by fluorescence spectrophotometer (Cary eclipse, Agilent Technologies, USA). Cell fluorescence images were captured by confocal laser scanning microscopy (TCS SP8, Leica, Germany) and Cytation 5 imaging reader (BioTek, USA). The

gels were imaged with chemiluminescence imaging system (ChemiDoc, Bio-Rad, USA). Flow cytometry analysis was conducted by flow cytometer (CytoFLEX S, Beckman, USA). Cell viability was measured by using Multiskan GO (Thermo Scientific, USA). 660 nm laser irradiation (Hi-Tech Optoelectronics Co., Ltd., China) was used for photodynamic therapy.

Rolling cycle amplification template design. The template (71 bases) for ADMP was consists of a sequence complementary to the AS1411 sequence (blue) and a sequence complementary to the c-Myc DNzyme sequence (green). The details were shown in **Table S1**.

Preparation of DNA nanoassemblies aptamer DNzyme@MnO₂@photosensitizer (ADMP). The synthesis of MnO₂ NPs was based on the previous report.¹ Briefly, 250 mg of BSA was dispersed in 7 mL of ultrapure water. Then, 31.6 mg of KMnO₄ dispersed in 3 mL of ultrapure water was dropwise added. The whole reaction was processed at 37 °C for 2 h. The obtained MnO₂ NPs were purified by dialysis using the dialysis bag with a cut-off molecular weight of 8–14 kDa. Then the purified nanoparticles were stored at 4 °C for the following use. The synthesis of aptamer DNzyme@MnO₂@photosensitizer (ADMP) was carried out by the following steps. A phosphorylated linear ssDNA (2 μM) and a primer (4 μM) were mixed and annealed to form a circular DNA template in DNA ligation buffer (10 mM Tris-HCl, 2 mM MgCl₂, 2 mM dithiothreitol, and 0.2 mM ATP) by heating at 95 °C for 5 min, followed by gradual cooling to room temperature over 4 h. The annealed product was chemically connected by adding T4 DNA ligase (10 U μL⁻¹) at 20 °C for 4 h.^{2,3} For rolling circle amplification (RCA), the resultant circularized template (1 μM) was incubated with TMPyP4 (0.1 mM), MnO₂ (1 mg mL⁻¹), phi29 DNA polymerase (1 U μL⁻¹) and dNTP (1 mM) in the reaction buffer (50 mM Tris-HCl, 10 mM (NH₄)₂SO₄, 10 mM MgCl₂ and 4 mM dithiothreitol). The reaction solution was incubated at 30 °C for 3 h and terminated by holding at 75 °C for 10 min. The obtained ADMP was then washed with ultrapure water three times by centrifuged at 10000 rpm for 10 min and stored at 4 °C for future use. To synthesize the Cy5-modified nanoassemblies, Cy5-dCTP (10 μM) was introduced to the RCA reaction mixtures to synthesize for fluorescence imaging.

Calculation of replicated copies of DNA nanoassemblies. Generally, the concentration of dNTP and nucleotides of the circle template were known in this reaction system. Thus, the consumed dNTP in the RCA reaction could be measured. The replication efficiency of the DNA could be calculated by the following equation:

$$\text{DNA copies} = (C_{\text{dNTP}} \times 4 - \text{OD}_{260}/\varepsilon \times 100) \times 1000 / (N_{\text{template}} \times C_{\text{template}}) \quad (1)$$

where C_{dNTP} and C_{template} represent the concentration of dNTP and template, respectively, OD_{260} represents the absorbance of the supernatant at $\lambda = 260$ nm, ε represents the extinction coefficient of dNTP, N_{template} represents the number of nucleotides in template. The calculation details can be seen in **Table S2**.

PAGE analysis. The molecular weight of linear ssDNA, primer and DNA nanoassemblies were investigated by native polyacrylamide gel electrophoresis (PAGE). The samples were mixed with $6 \times$ loading buffer and transferred into the 12% native polyacrylamide gel. Then, the electrophoresis was performed at a constant potential of 110 V in $1 \times$ TBE buffer (89 mM Tris, 89 mM boric acid, 2.0 mM EDTA, pH 8.3) for 1 h. After staining in diluted Gel-Red solution for 20 min, the gel was imaged by ChemiDoc (BIORAD, USA) under 365 nm UV irradiation.

Calculation of TMPyP4 concentration, loading capability, and encapsulation efficiency.

After RCA, the DNA nanoassemblies were washed with ultrapure water and gathered by centrifuged at 10000 rpm for 10 min. The free TMPyP4 in the supernatant was quantified by measuring the absorption of TMPyP4 at 425 nm *via* UV-vis spectroscopy. The TMPyP4 loading concentration, loading capability, and encapsulation efficiency were calculated by the following equations:

$$\text{Loading capability } C_{\text{loaded}} = (N_{\text{total}} - C_{\text{supernatant}} \times V_{\text{supernatant}}) / V_{\text{RCA}} \quad (2)$$

$$\text{Loading capability (\%)} = M_{\text{loaded}} / (M_{\text{loaded}} + M_{\text{DNA}}) \times 100\% \quad (3)$$

$$\text{Encapsulation efficiency (\%)} = C_{\text{loaded}} / C_{\text{total}} \times 100\% \quad (4)$$

where N_{total} represents the total molar amount of TMPyP4, $C_{\text{supernatant}}$ represents the concentration of TMPyP4 in the supernatant, and $V_{\text{supernatant}}$ and V_{DNA} represent the volume of the supernatant and the DNA nanoassemblies reaction buffer, respectively. M_{loaded} and M_{DNA} represent the weight of loaded TMPyP4 and DNA nanoassemblies, respectively. C_{loaded} and C_{total} represent the concentration of the loaded TMPyP4 and total amount TMPyP4, respectively. The details can be seen in **Table S4**.

***In vitro* cleavage reactions.** The cleavage efficiency of the DNA nanoassemblies was evaluated by denatured polyacrylamide gel electrophoresis (PAGE) and fluorescent spectra. Firstly, DNA nanoassemblies aptamer DNAzyme (AD) was incubated with substrate for 1 h in Tris-HCl buffer (50 mM, pH 7.5, containing 150 mM NaCl). Then, the exogenous Mn^{2+} ions and Mg^{2+} ions were added into the above mixture to activate the DNAzyme-mediated cleavage reaction,

respectively. Besides, nanoassemblies AD and aptamer DNAzyme@MnO₂ (ADM) were preincubated in acetate buffer (pH 5.0) with H₂O₂ for 1 h to degrade MnO₂, respectively. Subsequently, Tris-HCl (50 mM, pH 7.4, 150 mM NaCl) was used to adjust the pH, and the substrate was added into the buffer to explore the cleavage reaction at 37 °C for 3 h.

Measurement of MnO₂ degradation. ADMP were dispersed in different pH values (7.4 and 5.0) Tris-HCl buffer with or without H₂O₂. At the given time points, the solution was measured by UV-vis spectrometer for characterizations.

Measurement of oxygen generation. MnO₂ was able to react with H₂O₂ to generate oxygen (O₂) in the acid H₂O₂-rich tumor microenvironment. Briefly, the different DNA nanoassemblies samples were added into PB buffer (pH = 5.0) with H₂O₂, respectively. The time-dependent generation of oxygen generation was immediately recorded by a portable dissolved oxygen meter (JPSJ-605F Dissolved Oxygen Meters)

Measurement of singlet oxygen generation. The capability of ADMP to sensitize formation of ¹O₂ upon photoexcitation was investigated using the 1,3-diphenylisobenzofuran (DPBF)-based spectroscopic method and X-band electron spin resonance (ESR) with the spin traps 2,2,6,6-tetramethylpiperidine (TEMP). For ESR measurements, different materials were mixed with TEMP. Then, the mixtures were irradiated by 660 nm laser (0.2 W cm⁻²) for 5 min. Triplet signals were detected by the electron spin resonance (ESR) spectroscopy. To exclude the possible generation of other ROS, TMPyP4 was mixed with 5,5-Dimethyl-1-pyrroline N-oxide (DMPO) for detection. For the DPBF-based spectroscopic method, DPBF ethanol solution (20 mM, 10 μL) was added to different pH values (pH 7.4 and 5.0) ADMP (equal to 5 μM of TMPyP4, 1mL) PB-ethanol (v/v = 4:6) mixed solution with or without the addition of H₂O₂ (100 μM). The PB buffer (pH 7.4) served as a control. To compare the ¹O₂ generation efficiency of bare TMPyP4, AD, ADM, ADP and ADMP, DPBF ethanol solution (20 mM, 10 μL) was added to different materials in pH 5.0 with H₂O₂ (100 μM). The reaction was irradiated with a 660 nm laser (0.2 W cm⁻²) in the dark, and the 410 nm absorption peak of DPBF was monitored every 30 s.

Stability analysis. The stability of ADMP was observed by DLS and native PAGE. The sample was incubated with PBS (pH = 7.4), DNase I (1 U mL⁻¹), DMEM (10% serum) at 37 °C for 24 h, respectively.

Cell culture. All cells were purchased from Cell Bank of Chinese Academy of Sciences in Shanghai. Murine breast cancer cells (4T1) were cultured in a DMEM medium containing 10% fetal bovine serum (FBS) and 1% streptomycin/penicillin, while human breast normal cells (MCF-10A) were cultured with a special medium for MCF-10A cells. The culture conditions of the two kinds of cells were at 37 °C in a humid environment with 5% CO₂. For mimicking the hypoxic tumor microenvironment, 4T1 cells were cultured in a DMEM medium in an atmosphere with 1% O₂ and 5% CO₂ at 37 °C.

Cell uptake. To examine the cellular uptake capacity of DNA nanoassemblies ADMP, 4T1 cells were seeded in 12-well plates at a density of 5×10^4 cells per well overnight. Subsequently, the Cy5-labeled ADMP was added into the cells and incubated for different times (0 h, 1 h, 2 h, 4 h, 6 h, 8 h, or 10 h). The uninternalized Cy5-labeled DNA nanoassemblies were washed away with PBS three times, and the cells were digested by 0.25%-trypsin-EDTA and subjected to flow cytometry.

To verify the targeting effect of the AS1411 aptamer on ADMP, 4T1 cells and MCF-10A cells were seeded in confocal culture dishes (1×10^4 cells per dish) overnight, respectively. After attachment, the cells were incubated with Cy5-ADMP at 37 °C for 8 h. After the uninternalized DNA nanoassemblies were removed, the cells were treated with 4% paraformaldehyde and DAPI, then observed by confocal laser scanning microscope (CLSM).

To prove the targeting performance of AS1411 more directly, 4T1 cells were seeded in confocal dishes (2×10^4 cells per dish) overnight. After attachment, the cells were preincubated with or without the addition of excess free aptamer AS1411 (5 μM) at 37 °C for 1 h and washed three times with PBS immediately. The cells were further incubated with Cy5-ADMP at 37 °C for 8 h. After the uninternalized DNA nanoassemblies were removed, the cells were stained with DAPI and observed by CLSM.

Colocalization analysis. 4T1 cells were seeded in confocal dishes (2×10^4 cells per dish) overnight at 37 °C. After attachment, the cells were incubated with Cy5-ADMP for different times (6 h or 8 h) and washed three times with PBS immediately. After the uninternalized DNA nanoassemblies were removed, the cells were further stained with LysoTracker Green (5 μM) for 30 min at 37 °C and observed by CLSM.

Quantitative reverse-transcription polymerase chain reaction (qRT-PCR). 4T1 cells (1×10^5 cells per well) were seeded in 6-well plates overnight. Subsequently, the cells were treated

with PBS, AmutD, AmutDM, AD, ADM (equal to 40 $\mu\text{g mL}^{-1}$ of DNA nanoassemblies) for 48 h, respectively. Total RNA was extracted with a HP total RNA Kit (Omega) according to the manufacturer's instructions. The cDNA was synthesized from 1 μg of RNA using the PrimeScript first-strand cDNA synthesis kit (Bio-Rad). Real-time PCR was performed using the CFX Connect real-time PCR Detection System (Bio-Rad). Relative gene expressions were calculated using the $2^{-\Delta\Delta\text{Ct}}$ method.

The sequences of PCR primers are listed as follows:

c-Myc forward primer: 5'-CAAGAGGCGAACACACCACGTCT-3'

c-Myc reverse primer: 5'-CCACATACAGTCCTGGATGAT-3'

Western blot assay. The cells were pretreated in the same way as qRT-PCR, followed by washing two times with precooled PBS. The proteins were obtained by using RIPA Lysis buffer and centrifuged at 14000 g for 10 min at 4 °C. The supernatants were collected, separated by sodium dodecyl sulfate polyacrylamide gel electrophoresis (SDS-PAGE), and then transferred to the nitrocellulose (NC) membrane (Invitrogen, USA). The membranes were blocked with 5% BSA in the PBST solution and blotted with antibodies against α -tubulin (3873S, Cell Signaling Technology, 1:1000) and c-Myc (5605S, Cell Signaling Technology, 1:1000). Next, the membrane was incubated with secondary antibody (7076S, Cell Signaling Technology, 1:1000) for 1 h and detected using a Bio-Rad imaging system (ChemiDoc).

Measurement of intracellular singlet oxygen generation. DCFH-DA was employed to evaluate the intracellular $^1\text{O}_2$ generation after light illumination. Briefly, 4T1 cells were seeded in 12-well plates (1×10^5 cells per well) overnight. After that, cells were treated with PBS, AmutDP, AmutDMP (equal to 40 $\mu\text{g mL}^{-1}$ of DNA nanoassemblies) for 8 h under normoxic and hypoxic conditions respectively, followed by washing three times and incubating with DCFH-DA solution (10 μM in the DMEM without FBS) at 37 °C for 20 min. After removal of the DCFH-DA solution and washing with PBS buffer, the cells were exposed to a 660 nm laser (0.2 W cm^{-2} , 5 min). The fluorescence images of the cells were immediately captured by a Cytation 5 imaging reader.

Cytotoxicity assay. Cell cytotoxicity was measured by the classic cell counting kit-8 (CCK-8) method under normoxia (21% oxygen) or hypoxia (1% oxygen). 4T1 cells were seeded in 96-well plates (2.5×10^3 cells per well) overnight. Subsequently, the cells were incubated with PBS, AD, ADM, AmutDP, AmutDMP, or ADMP (equal to 40 $\mu\text{g mL}^{-1}$ of DNA

nanoassemblies) for 8 h under normoxic and hypoxic conditions, respectively. After that, the cells were exposed to a 660 nm laser (0.2 W cm^{-2} , 5 min) for photodynamic therapy groups, and then all groups were further incubated for 40 h. Before testing, the cells were treated with 10 μL CCK-8 reagents at 37 °C for 2 h in dark *via* the protocol. The optical density (OD) value at 450 nm of the resulting solution was obtained by using the microplate reader. The cell viability was calculated as follows:

$$\text{Cell viability (\%)} = (\text{OD}_{\text{Samples}}/\text{OD}_{\text{PBS}}) \times 100\% \quad (5)$$

Where $\text{OD}_{\text{Samples}}$ and OD_{PBS} represent the OD value at 450 nm after different materials and PBS treatments.

Annexin V/PI assay. The apoptotic cells were investigated by annexin V-FITC and PI double staining. Generally, 4T1 cells were seeded in 12 well plates (5×10^4 cells per well) overnight and then incubated with PBS, AD, ADM, AmutDP, AmutDMP, or ADMP (equal to $40 \mu\text{g mL}^{-1}$ of DNA nanoassemblies) for 8 h. The cells of photodynamic therapy groups were irradiated with a 660 nm laser (0.2 W cm^{-2} , 10 min). After further incubating for 40 h and washing three times with PBS buffer, the 4T1 cells were digested by trypsin (without EDTA), resuspended in 500 μL of annexin binding buffer, and stained with 5 μL of annexin V-FITC for 15 min and 10 μL of PI for 5 min. Subsequently, the apoptosis rate was tested by flow cytometry.

Live/Dead cell staining assay. 4T1 cells were seeded in 12-well plates (5×10^4 cells per well) overnight. Then 4T1 cells were incubated with PBS, AD, ADM, AmutDP, AmutDMP, or ADMP (equal to $40 \mu\text{g mL}^{-1}$ of DNA nanoassemblies) for 8 h. For photodynamic therapy groups, the cells were exposed to a 660 nm laser (0.1 W cm^{-2} , 10 min). After incubating for another 40 h and washing three times with PBS solution, the 4T1 cells were stained with Calcein-AM (4 μM) and PI solutions (4 μM) in PBS and incubated for 30 min. Finally, the cells were observed *via* Cytation™ 5 Cell Imaging Multi-Mode4 Reader.

Hemolysis assay. Red blood cells were obtained by centrifuging fresh mouse blood at 5,000 rpm for 5 min, washed with PBS, and then diluted with a proper amount of PBS. Next, a total of 0.2 mL of the red blood cells (RBCs) was added to 0.8 mL of materials at different concentrations ($5\text{-}40 \mu\text{g mL}^{-1}$). PBS and deionized water were set as negative and positive controls, respectively. After being stationary at 37 °C for 4 h, the samples were centrifuged at 10000 rpm for 5 min, and the supernatant was obtained to access the absorbance at 570 nm by a microplate reader and calculate the hemolysis ratio.

The hemolysis (%) was calculated by the following equation:

$$\text{Hemolysis (\%)} = (A_{\text{sample}} - A_{\text{negative}})/(A_{\text{positive}} - A_{\text{negative}}) \times 100\% \quad (6)$$

where A_{sample} represents the absorbance of supernatant after incubation of blood and materials, A_{negative} and A_{positive} represent the absorbances of supernatant after incubation of PBS and H₂O, respectively.

Tumor mouse model. All animal experiments were carried out following the Animal Care and Use Committee of Wuhan University. The animal protocol was approved by the Use Committee of the Animal Experiment Center/Animal Biosafety Level-III Laboratory of Wuhan University (license number: WP20210450). 1×10^6 4T1 cells in 50 μL PBS-Matrigel (v/v = 1:1) were injected into the in the backs of the BABL/c female mice (4-5 weeks). The tumors were allowed to grow for 5 days or until the tumor size reached 100-150 mm^3 before being used for fluorescence imaging and therapeutic experiments. The tumor volume (V) was measured by digital calipers and calculated by the following equation:

$$V = W^2 \times L/2 \quad (7)$$

in which W and L represent the shortest and longest diameters of tumors, respectively.

In vivo fluorescence imaging. When the tumor volume reached about 150 mm^3 , 50 μL Cy5-conADMP and Cy5-ADMP (corresponds to 3.66 mg kg^{-1} of DNA nanoassemblies) were injected into 4T1 tumor-bearing mice through the tail vein. At 4 h, 8 h 12 h, and 24 h post-injection, fluorescence images of live mice were collected with an IVIS Lumina XRMSIII *in vivo* imaging system (Caliper Life Science, USA).

In vivo antitumor assay. Treatments were performed when tumor volumes reached about 100 mm^3 . Subsequently, the mice were randomly divided into seven groups (five mice per group). Each group was injected with 50 μL different materials (corresponds to 3.66 mg kg^{-1} of DNA nanoassemblies) twice a week through tail-vein injection: PBS (I), AmutDMP (II), AD (III), ADM (IV), AmutDP with laser (V), AmutDMP with laser (VI), or ADMP with laser (VII). After intravenous injection for 12 h, the PDT groups were irradiated with a 660 nm laser (0.2 W cm^{-2} , 10 min).

To investigate the therapeutic effects, the tumor volume and body weight were measured every two days. On the 15th day, all the animals were sacrificed, the major organs (heart, liver, spleen, lung, and kidney) and tumors were excised and collected for further analysis.

Immunofluorescence stainings of c-Myc. To further study the excellent down-regulating expression of c-Myc, the tumors were excised and collected on the 15th day. Then the tumors of mice with different groups were fixed in 4% formalin and then embedded in paraffin for c-Myc staining.

H&E and TUNEL staining. On the 15th day, the heart, liver, spleen, lung, kidney, and tumor tissues harvested from every group of mice were fixed in 10% paraformaldehyde solution and then embedded in paraffin to collect slices for H&E staining. To investigate tumor cell apoptosis, tumors were also stained for TUNEL. Images were acquired using a Cytation™ 5 Cell Imaging Multi-Mode4 Reader.

Blood biochemical assay. After various treatments, blood samples (200 μ L, n = 3) were obtained by pulling out the eyeball. The serum was obtained through centrifugation at 5000 rpm for 5 min. Blood levels of haemoglobin (HGB), albumin (ALB), total protein (TP), urine acid (UA), creatinine (CRE), blood urea nitrogen (BUN), alanine aminotransferase (ALT), and aspartate aminotransferase (AST) were measured by using the commercial kits.

Statistical analysis. Statistical significance was calculated by one-way ANOVA with Tukey's post hoc test: *** $p < 0.001$, ** $p < 0.01$, * $p < 0.05$.

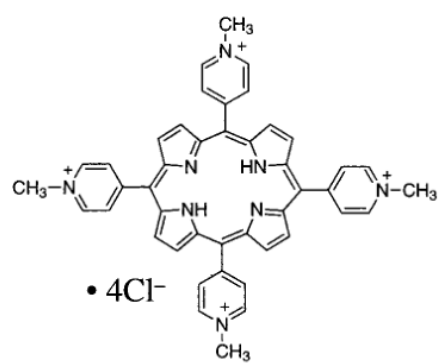


Fig. S1 Structure of porphyrin photosensitizer (TMPyP4).⁴

Table S1. DNA sequences.

Name	Sequence (5'→3')
	Phosphate-
AD Template	GTCACGACGTCGTTGTAGCTAGCCTGCCCTCATT TTTTT CCAC CACCACCACAACCACCACCACCTTTTTT
	Phosphate-
AmutD Template	GTCACGACGTCGTTGTAG G TAGCCTGCCCTCATTTTTTT CCAC CACCACCACAACCACCACCACCTTTTTT
Prmer1	GACGTCGTGACAAAAAAGGTGG
	Phosphate-
conAD Template	GTCACGACGTCGTTGTAGCTAGCCTGCCCTCATTTTTTT CCCT AAC CCCTAACCC TAA CCCTAA TTTTTT
Prmer2	GACGTCGTGACAAAAAATTAGG

Green letters: Complementary to DNzyme sequence; **Blue letters:** Complementary to aptamer sequence; **Red letter:** mutant base.

Table S2. DLS measurement of different nanoassemblies.

Sample	Z-Average (nm)	PDI
MnO₂	8.8 ± 0.9	0.377
AD	359.7 ± 5.5	0.213
ADM	365.1 ± 10.3	0.179
ADMP	366.2 ± 8.3	0.119

Table S3. Calculation of replicated copies of DNA nanoassemblies.

	Notes	AD	ADM	ADMP
Total dNTP concentration (C_{total})	2 mM for each	8 mM	8 mM	8 mM
OD₂₆₀ of remnant dNTP	100 × dilution	0.22	0.17	0.27
Average extinction coefficient of dNTP (cm M)⁻¹	ϵ	11950	11950	11950
Remnant dNTP concentration (C_{remnant})	$OD_{260}/\epsilon \times 100$	1.84 mM	1.42 mM	2.23 mM
Consumed dNTP (C_{consumed})	$C_{\text{total}} - C_{\text{remnant}}$	6.16 mM	6.58 mM	5.74 mM
Number of nucleotides in template	N_{template}	71	71	71
Average replicated copies for each template (1 μM of template)	$C_{\text{consumed}} \times$ $1000/(N_{\text{template}} \times$ $1)$	87	93	81

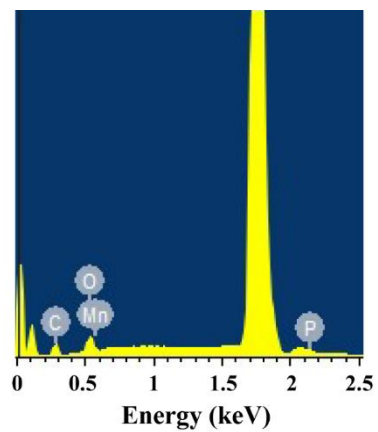


Fig. S2 Energy dispersive X-ray spectroscopy (EDX) of ADMP.

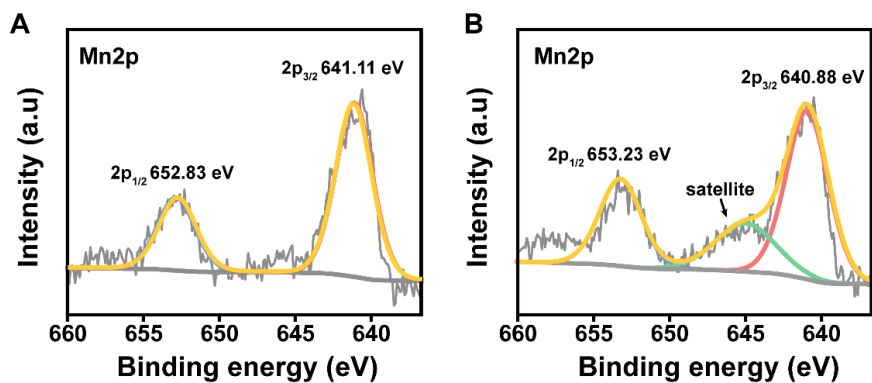


Fig. S3 X-ray photoelectron spectroscopy (XPS) of ADMP without (A) or with (B) acidic H₂O₂.

Discussion: The split energy between Mn 2p_{3/2} (641.11 eV) and Mn 2p_{1/2} (652.83 eV) was 11.72 eV, which indicated that the oxidation state of Mn was mainly +4. After reaction of ADMP with acidic H₂O₂, the split energy between Mn 2p_{3/2} (640.88 eV) and Mn 2p_{1/2} (653.23 eV) was 12.35 eV, and the satellite feature was observed, which indicated the generation of Mn²⁺.

Table S4. Calculation of photosensitizer loading capability and encapsulation efficiency.

Name	Notes	ADMP
Concentration of employed TMPyP4 (C_{total})	/	100 μM
Total volume of reaction solution (V_{RCA})	/	100 μL
OD₄₂₅ of remnant TMPyP4	5 \times dilution	0.1
Standard curve of TMPyP4	$y = 0.218x - 0.032$	/
Concentration of supernatant TMPyP4 ($C_{\text{supernatant}}$)	$(\text{OD}_{425} + 0.032)/0.218 \times 5$	2.87 μM
Volume of supernatant TMPyP4 ($V_{\text{supernatant}}$)	All supernatants in the purification process were collected	300 μL
Concentration of loaded TMPyP4 (C_{loaded})	$C_{\text{total}} - C_{\text{supernatant}} \times 3$	91.4 μM
Drug encapsulation efficiency (%)	$C_{\text{loaded}}/C_{\text{total}} \times 100\%$	91.4
Mass of loaded TMPyP4 (m_{loaded})	$M = 1363.6 \text{ g mol}^{-1}$	0.012 mg
Mass of DNA nanoassemblies (M_{DNA})	/	0.093 mg
Drug loading capacity (%)	$M_{\text{loaded}}/(M_{\text{loaded}} + M_{\text{DNA}}) \times 100\%$	11.4

Table S5. DLS analysis of ADMP with different treatments for 24 h.

Treatment	Z-Average (nm)	PDI
PBS	343.3 ± 7.3	0.158
DNase I (1 U mL⁻¹)	345.9 ± 13.4	0.139
DMEM (10% serum)	349.0 ± 14.3	0.231

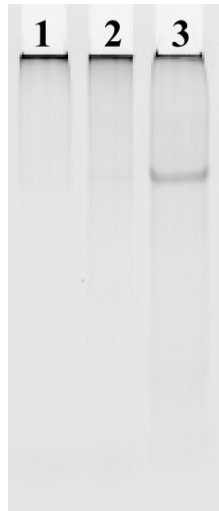


Fig. S4 Native PAGE analysis of ADMP incubated with PBS (Line 1), DNase I (1 U mL^{-1}) (Line 2), and DMEM (10% serum) (Line 3) for 24 h.

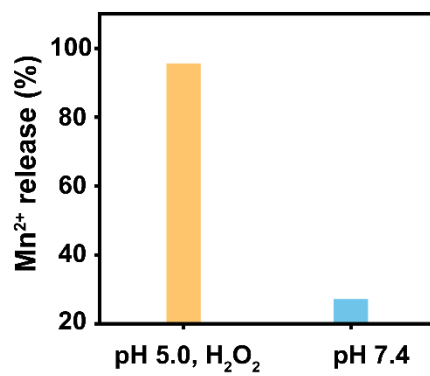


Fig. S5 ICP-MS analysis of Mn²⁺ release from ADMP in different media.

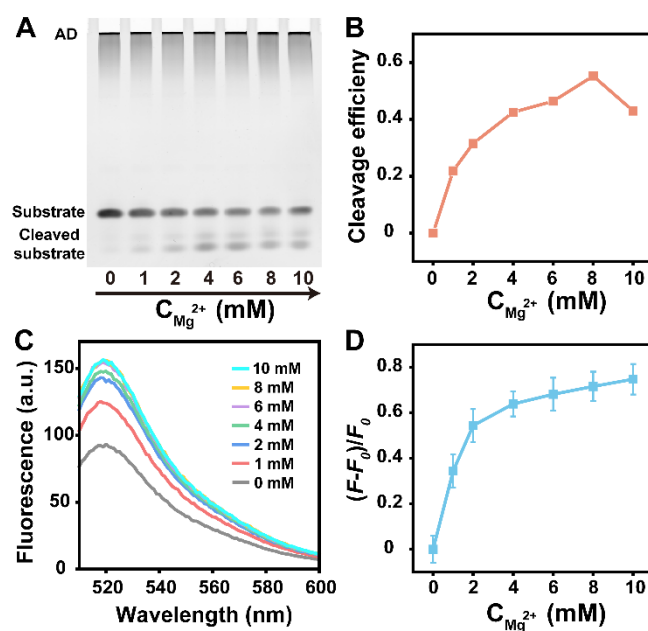


Fig. S6 (A) Denatured PAGE analysis of DNazyme-mediated AD cleavage with different concentrations of Mg^{2+} ions. (B) Cleavage efficiency of the AD with different concentrations of Mg^{2+} ions as shown in Fig. S4A. (C) Fluorescence spectra generated by DNazyme-mediated AD cleavage in the presence of different concentrations of Mg^{2+} ions. (D) The corresponding fluorescence intensity changes (at $\lambda=520$ nm) as shown in Fig. S4C.

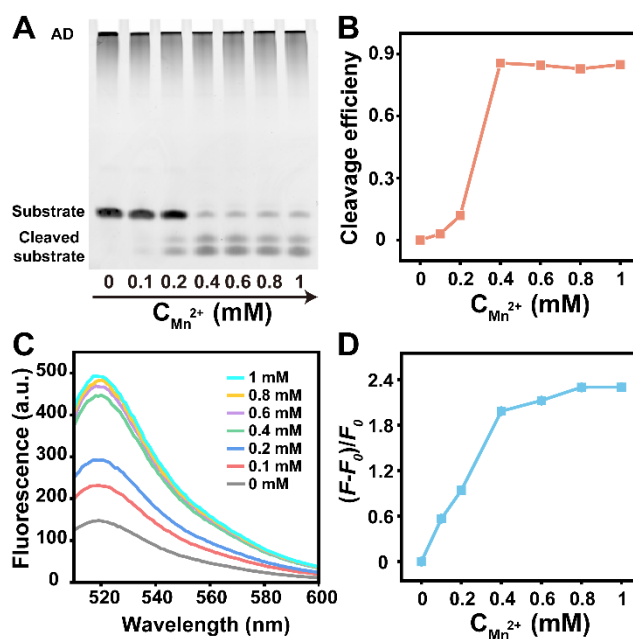


Fig. S7 (A) Denatured PAGE analysis of DNAzyme-mediated AD cleavage with different concentrations of Mn^{2+} ions. (B) Cleavage efficiency of the AD with different concentrations of Mn^{2+} ions as shown in Fig. S5A. (C) Fluorescence spectra generated by DNAzyme-mediated AD cleavage in the presence of different concentrations of Mn^{2+} ions. (D) The corresponding fluorescence intensity changes (at $\lambda=520$ nm) as shown in Fig. S5C.

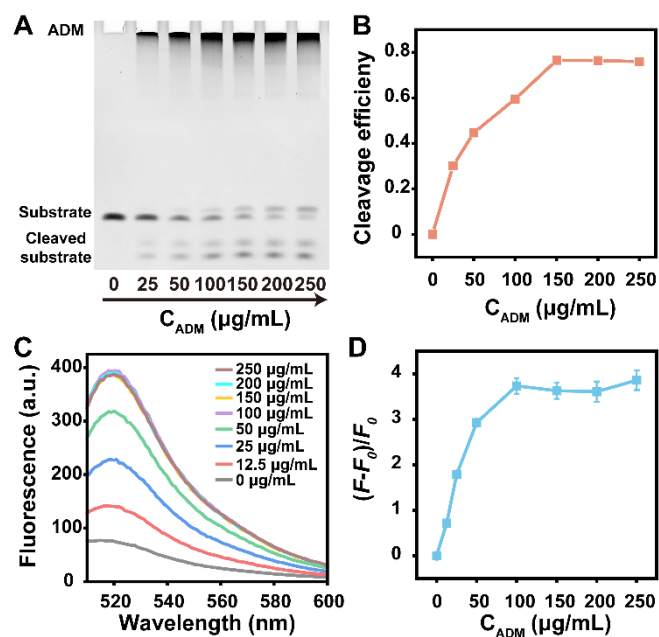


Fig. S8 (A) Denatured PAGE analysis of DNAzyme-mediated ADM cleavage with different concentrations ADM. (B) Cleavage efficiency of different concentrations of ADM as shown in Fig. S6A. (C) Fluorescence spectra generated by DNAzyme-mediated ADM cleavage in the presence of different concentrations of ADM. (D) The corresponding fluorescence intensity changes (at $\lambda=520$ nm) as shown in Fig. S6C.

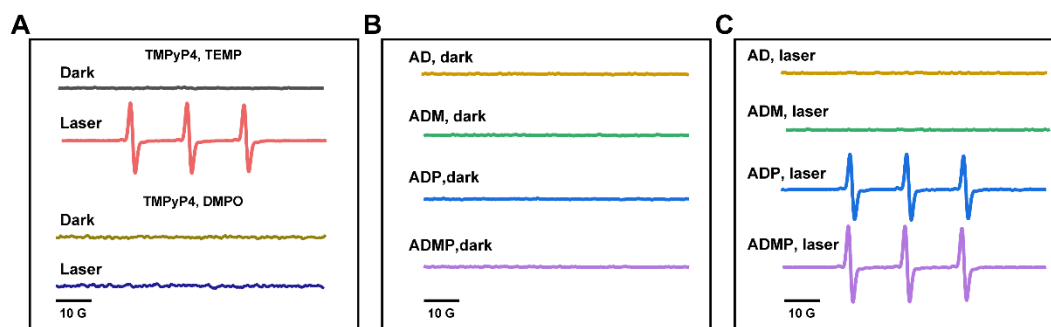


Fig. S9 (A) ESR analysis of the type of ROS species generated from TMPyP4. (B-C) ESR spectra of different materials before (A) and after (B) laser irradiation by using TEMP as the trapping agent.

Discussion: Upon laser irradiation, the ESR spectrum of TMPyP4 clearly display 1:1:1 triplet signal characteristic, which indicated that TMPyP4 could catalyze the generation of $\cdot^1\text{O}_2$. In addition, 5,5-Dimethyl-1-pyrroline N-oxide (DMPO) has been used as spin trap agent to exclude the possible generation of other ROS generated by TMPyP4, and no other ROS signals are detected. Similarly, significant 1:1:1 triplet signal characteristic can be observed in ADP and ADMP under laser irradiation, which also indicated the generation of $\cdot^1\text{O}_2$.

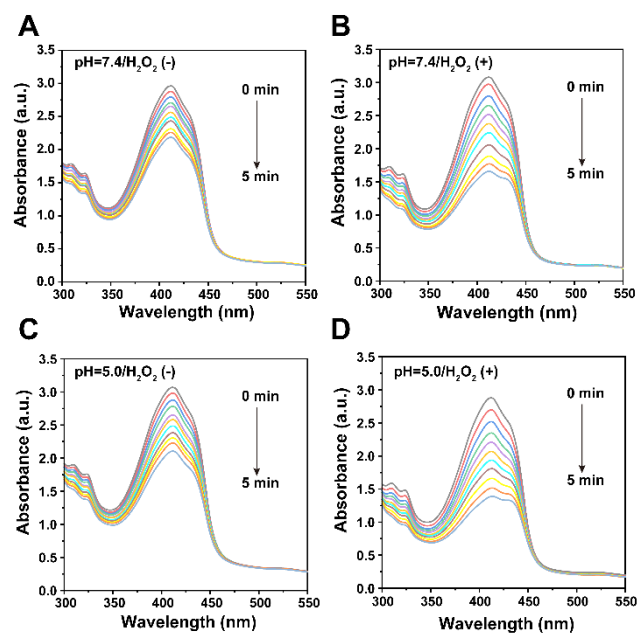


Fig. S10 UV-vis absorption spectra of DPBF with ADMP in the presence/absence of 100 μM H_2O_2 at pH 5.0 or 7.4 at various irradiation times, respectively.

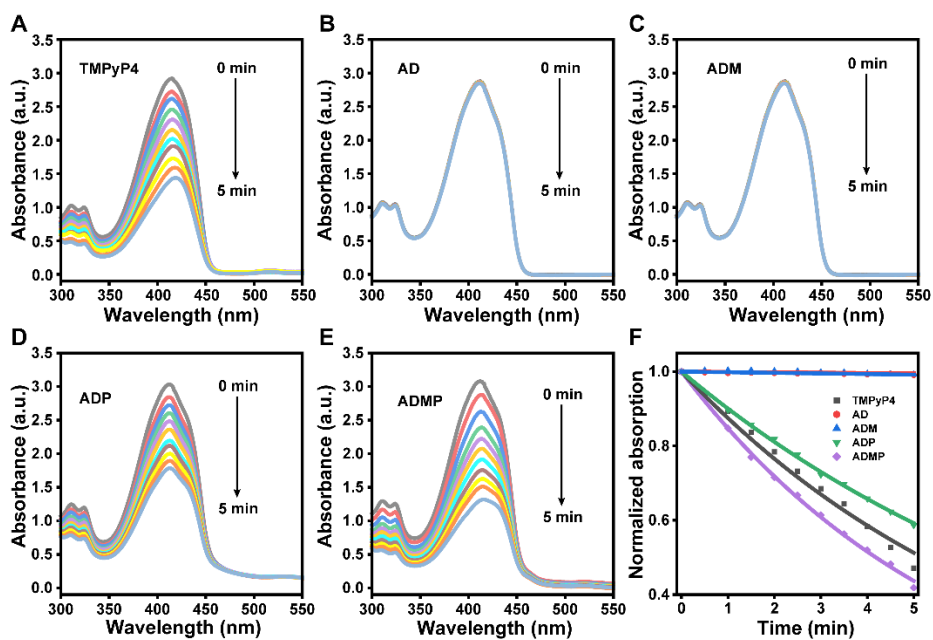


Fig. S11 $^1\text{O}_2$ generation efficiency measurements. (A-E) UV-vis spectrum of DPBF with TMPyP4 (A), AD (B), ADM (C), ADP (D), and ADMP (E) at various irradiation times. (F) Consumption of DPBF over irradiation times due to $^1\text{O}_2$ generation by TMPyP4, AD, ADM, ADP and ADMP under 0.2 W cm^{-2} of 660 nm laser irradiation.

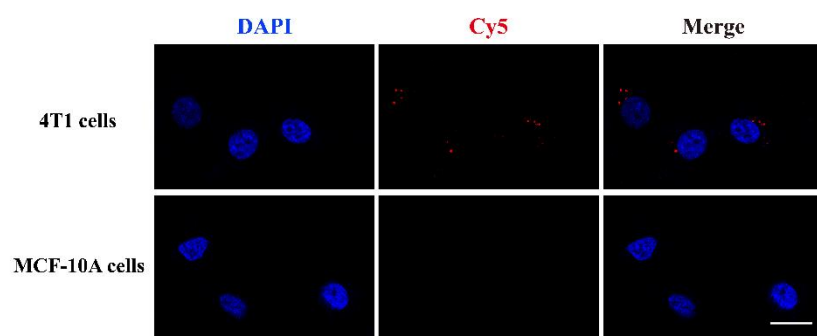


Fig. S12 Confocal fluorescence images of 4T1 and MCF-10A cells that were incubated with Cy5-labeled ADMP separately. Scale bar, 20 μm .

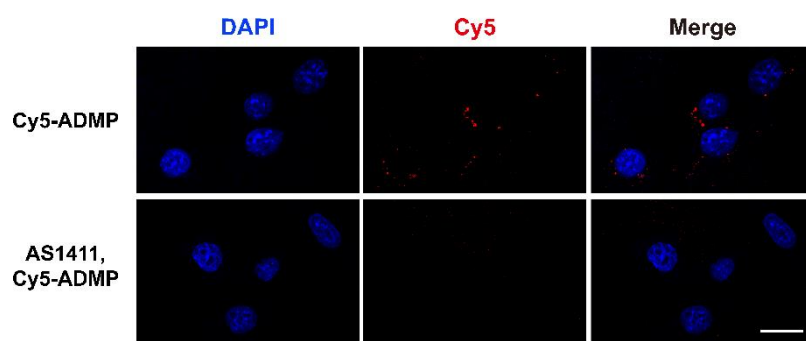


Fig. S13 Confocal fluorescence images of 4T1 cells that were incubated with or without excess free aptamer AS1411 before incubating with Cy5-labeled ADMP. Scale bar, 20 μm .

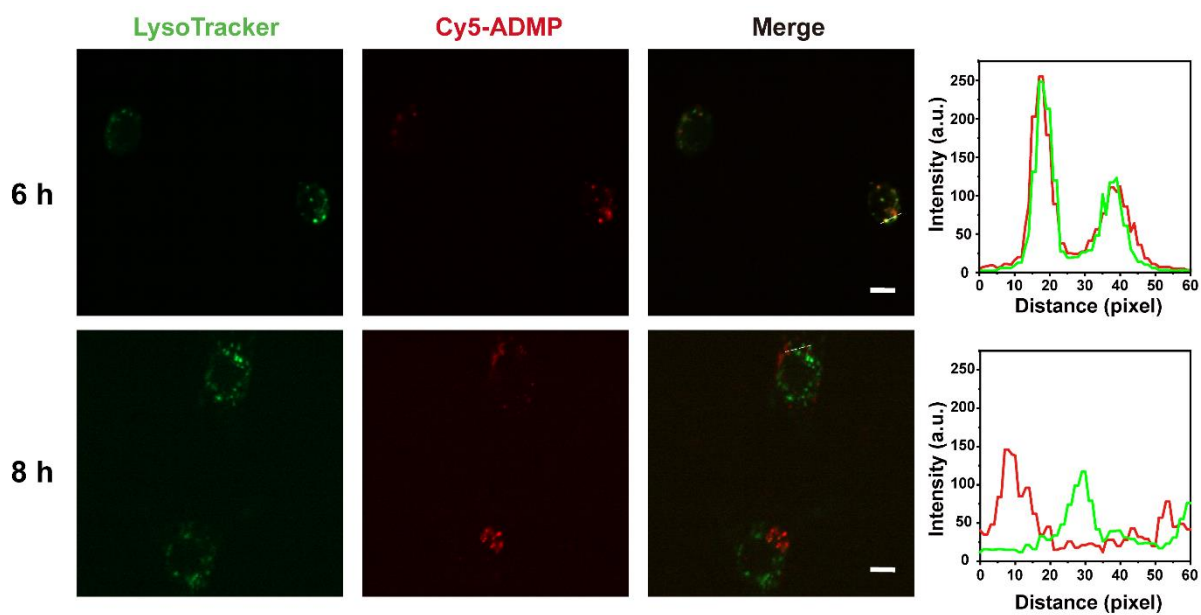


Fig. S14 Colocalization analysis of Cy5-labeled ADMP with lysosomes in 4T1 cells for different times. Lysosome was stained with LysoTracker Green. Scale bars, 10 μ m. The distribution profile on the specified white line is shown in the right panel.

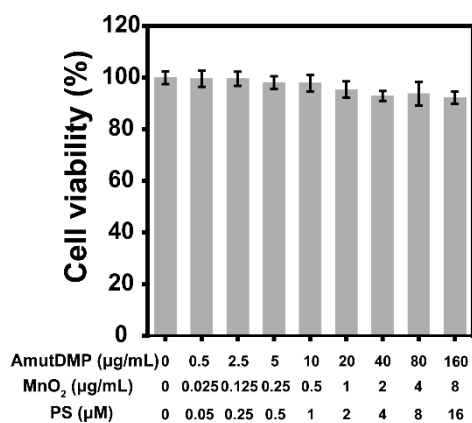


Fig. S15 Cell viability assay of 4T1 cells treated with different concentrations of non-photoirradiated AmutDMP for 48 h. Results are presented as means \pm standard deviation (SD) (n = 3).

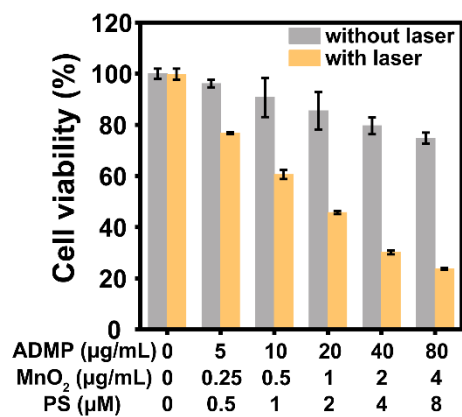


Fig. S16 Cell viability of 4T1 cells treated with different concentrations of ADMP with or without laser irradiation. The power of photoirradiation (660 nm) was 0.2 W cm^{-2} (5 min). Results are presented as means \pm standard deviation (SD) (n = 3).

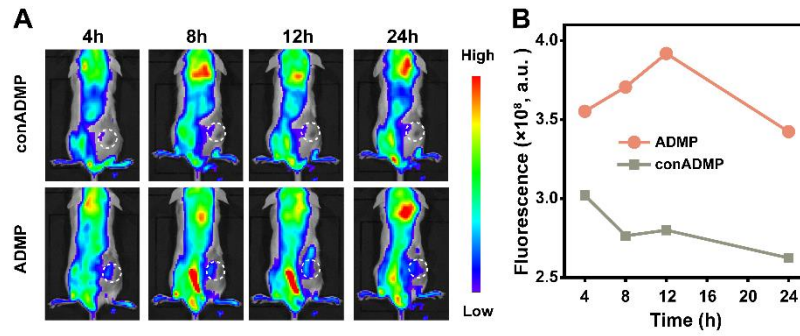


Fig. S17 (A) Fluorescence image and (B) quantitative analysis of 4T1 tumor-bearing mice after tail vein injection of Cy5-conADMP and Cy5-ADMP at different time points, respectively. Notably, aptamer-based active targeting accompany with EPR effects of passive targeting contributed to the increased permeation and the accumulation of ADMP at tumor tissues, although the size of ADMP is not ideal.

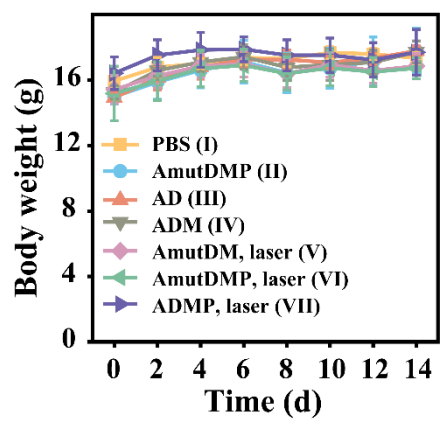


Fig. S18 Weight of mice with different treatments.

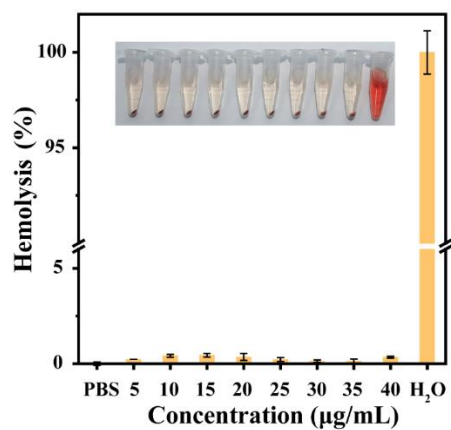


Fig. S19 Hemolysis test of ADMP at various concentrations. PBS and ultrapure water were used as the negative and positive control, respectively.

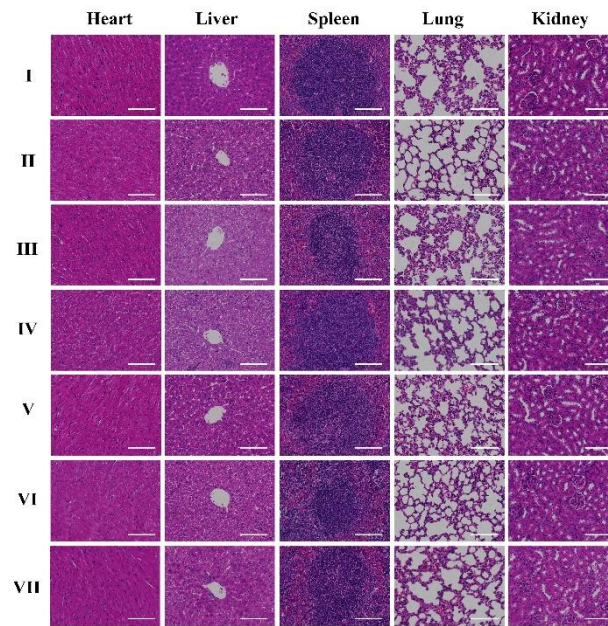


Fig. S20 Representative H&E staining images of major organs sections. The heart, liver, spleen, lung, and kidney of tumor-bearing mice with different treatments for 15 days. The mice were divided into seven groups: PBS (I), AmutDMP (II), AD (III), ADM (IV), AmutDP plus laser (V), AmutDMP plus laser (VI), and ADMP plus laser (VII). Scale bars, 100 μ m.

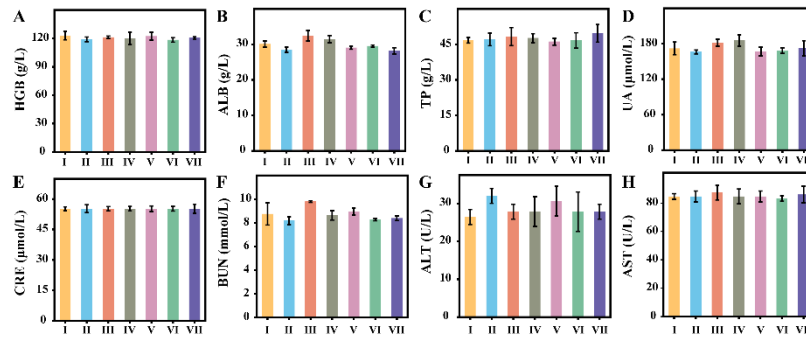


Fig. S21 Blood biochemical analysis of tumor-bearing mice with different treatments for 15 days. The investigated blood biochemical markers included (A) haemoglobin (HGB), (B) albumin (ALB), (C) total protein (TP), (D) urine acid (UA), (E) creatinine (CRE), (F) blood urea nitrogen (BUN), (G) alanine aminotransferase (ALT), and (H) aspartate aminotransferase (AST). The mice were divided into seven groups: PBS (I), AmutDMP (II), AD (III), ADM (IV), AmutDP plus laser (V), AmutDMP plus laser (VI), and ADMP plus laser (VII). Error bars denote mean \pm S.D. (n = 3).

References

- 1 J. Pan, Y. Wang, H. Pan, C. Zhang, X. Zhang, Y.-Y. Fu, X. Zhang, C. Yu, S.-K. Sun and X.-P. Yan, *Adv. Funct. Mater.*, 2017, **27**, 1603440.
- 2 J. Lee, J. Hong, D. Bonner, Z. Poon and P. Hammond, *Nat. Mater.*, 2012, **11**, 316-322.
- 3 Y. Lv, R. Hu, G. Zhu, X. Zhang, L. Mei, Q. Liu, L. Qiu, C. Wu and W. Tan, *Nat. Protoc.*, 2015, **10**, 1508-1524.
- 4 F. X. G. Han, R. T. Wheelhouse, L. H. Hurley, *J. Am. Chem. Soc.*, 1999, **121**, 3561-3570.